Title

fCO_2^{sw} variability in the Bay of Biscay during ECO cruises

Authors

Padín, X.A. [1], Castro, C.G. [1], Ríos, A.F. [1] and Pérez F.F. [1]

[1] Instituto de Investigaciones Marinas, CSIC, Eduardo Cabello, 6, 36208 Vigo, Spain

Corresponding e-mail address

padin@iim.csic.es

Abstract

The Bay of Biscay is part of the North Atlantic Ocean, the most important sink of CO_2, and a subduction zone of mode waters that favours the entry of carbon to the ocean interior. To investigate the seasonal and interannual variability of CO_2 uptake, continuous underway measurements of the partial pressure of CO_2 at sea surface were performed along a commercial route between Vigo (Spain) and St. Nazaire (France). An unattended measuring system of CO_2 fugacity (fCO_2), with meteorological station, and temperature, salinity, oxygen and fluorescence sensors, was installed on board of ships of opportunity (*RO-RO L'Audace* and *RO-RO Surprise*).

The dataset collected between December 2002 and December 2004 reported a significant interannual variability; mainly for the winter season. The noticeable increase of fCO_2^{sw} during the winter mixing period of 2004 was associated to biogeochemical differences related to nutrient ratios, phytoplankton activity and atmospheric CO_2 uptake. Dividing the seasonal cycle into three periods, prebloom (October – February),

bloom (March – May) and postbloom (June – September), the fCO_2^{sw} for the entire seasonal cycle was correctly predicted by empirical relationships with an error lower than 10 μatm in spite of the high interannual variability. The fCO_2^{sw} variability at seasonal scale was mainly controlled by processes of synthesis and remineralization of organic matter during prebloom and bloom periods whereas SST was the key parameter during postbloom period. The surface waters of the Bay of Biscay showed a clear role as atmospheric CO_2 sink ranging from -2.7±2.8 (±0.3) to -0.08±0.41 (±0.04) molC·m^{-2}·yr^{-1} (*mean*±*standard deviation* (±*error*)) throughout each complete period although CO_2 release to atmosphere was also observed during short episodes of summer. Using the regular wind speed sources of CO_2 fluxes estimation ranged from -1.3±1.7 (±0.1) to -2.4±2.7 (±0.1) molC·m^{-2}·yr^{-1} at annual scale, exceeding the sink capacity of the nearby regions of the North Atlantic Ocean.

51 INTRODUCTION

52

53 The world's oceans are currently a net sink for atmospheric CO_2 uptaking to almost
54 half of all fossil-fuel emissions (Sabine et al., 2004). The capacity of the oceans to
55 absorb the CO_2 excess plays a relevant role in the global warming mitigating the effect
56 of greenhouse gas emissions. Therefore quantification of oceanic CO_2 uptake is a key
57 for understanding the interactions and feedbacks between the carbon system and the
58 overall earth system. These interactions were the aim of multiple research programs in
59 the past decade (e.g. Tans et al., 1990; Sarmiento et al., 1995; Wallace, 1995; Gruber et
60 al., 1996; Brewer et al., 1997; Takahashi et al., 1997) but the exact magnitude of the
61 variability has not been completely constrained (Gruber et al., 2002; Watson et al.,
62 1991). The disagreements between ocean models (Le Quere et al., 2000) and
63 atmospheric inversions (Peylin et al., 2005) in relation to interannual variability of the
64 CO_2 global sink also emphasize the poorly constrained variability.

65

66 The knowledge of the ocean carbon cycle would improve by extending the CO_2
67 observations to larger areas for several years. Global carbon models (Sarmiento et al.,
68 1992; Maier-Reimer and Hasselmann, 1987) need appropriate dataset for model testing
69 or to assimilating in the new update models. To accomplish this objective, autonomous
70 CO_2 probes are increasing the frequency and spatial coverage of measurements.
71 Besides research vessels, ships of opportunity (Lüger et al., 2004; Padin et al., 2007
72 a,b), time series-stations (Gruber et al., 2002; Dore et al., 2003; Gonzalez-Davila et al.,
73 2003) and drifter buoys (Copin-Montégut and Avril, 1993; Lévy et al., 1998; Andersen
74 and Prieur, 2000; Hood and Merlivat, 2000) are becoming suitable platforms to develop
75 ambitious sampling strategies. Empirical algorithms are also used to extrapolate CO_2

partial pressure (pCO_2) observations in relation to even retrieved parameters from remote sensing (Tans et al., 1990; Metzl et al., 1995; Stephens et al., 1995; Goyet et al., 1998; Lee et al., 1998; Hood et al., 1999; Nelson et al., 2001; Lefevre and Taylor, 2002; Olsen et al., 2004).

A large part of these measurements has been carried out in the North Atlantic Ocean due to its outstanding role as CO_2 sink among oceanic regions (Takahashi et al., 2002). The formation of mode waters due to seasonally deep mixing and the notable phytoplankton activity yield the intense CO_2 absorption of the North Atlantic. Following these research efforts, our project (ECO: Evolution of CO_2 increase using ships of opportunity: Galician coast and Bay of Biscay) was developed with the aim of intensifying the CO_2 recordings in the Bay of Biscay. This regional sea has an important role in the subduction of mode waters in the North Atlantic Ocean (Paillet and Mercier, 1997) and represents one of the areas with the highest accumulation of anthropogenic CO_2 (Gruber, 1998).

In order to improve the description of the carbon cycle in the Bay of Biscay, an unattended measuring system of CO_2 fugacity (fCO_2) was installed on board of ships of opportunity. Additionally key physical and biological parameters were monitored to evaluate their relevance in the CO_2 variability at seasonal and interannual scale. Underway measurements were performed along 150 tracks from November 2002 to December 2004. The purpose of this work is to constrain the assessment of CO_2 flux as well as to describe the role of different drivers of fCO_2 distribution during ECO cruises.

MATERIALS AND METHODS

The dataset presented in this paper was collected on board of ships of opportunity from Flota Suardíaz Company (*RO-RO L'Audace* and *RO-RO Surprise*) between December 2002 and December 2004. he regular route linked Vigo (Spain) and St. Nazaire (France) with a frequency of 12 transects per month, measuring more than 150 tracks throughout two entire seasonal cycles.

Seawater was continuously pumped from 3 meters below waterline into the ship's hull. The volume of water was pumped at a high flow rate although a smaller flow was only shunted through the analytical system in order to reduce the warming of the water on the way. Afterwards the uncontaminated seawater supply was bifurcated to pass through an analytical system composed by thermosalinometer (SBE-45-MicroTSG), oximeter (SBE-43) and fluorometer (WETLabs) and through a home made fCO_2 analyser. The underway measurements of sea surface salinity (SSS), sea surface temperature (SST), oxygen (O_2) and chlorophyll *a* concentration (chl a) were recorded with CO_2 fugacity in seawater (fCO_2^{sw}) and atmosphere (fCO_2^{atm}).

The measurements of CO_2 mole fraction (xCO_2) were performed with a non-dispersive infrared gas analyser (LI-6262). This analyzer was calibrated at the beginning and end of each transit using two gases; one of CO_2-free air and one of high CO_2 standard gases with a certified concentration of ~375 ppm (Instituto Meteorológico Nacional, Izaña, Canary Islands).

xCO_2^{sw} was converted into fCO_2^{sw} in saturated water vapour pressure using the atmospheric pressure measured with the analysis unit as described in DOE Handbook

(1994). Subsequently fCO_2^{sw} values were corrected for the temperature shift by means of an empirical equation (DOE, 1994), originally proposed by Takahashi et al. (1993). The temperature difference between the seawater inlet and the equilibrator system was typically less than 1ºC.

During the ECO cruises atmospheric xCO_2 (xCO_2^{atm}) was measured every hour, recording twenty observations within 5 minutes. Subsequently, a selection criteria was applied to eliminate spurious values and to identify xCO_2^{atm} representative data. These data were fitted to a seasonal curve, consisting of an annual trend plus a seasonal cycle (Padin et al., 2007b). To convert xCO_2^{atm} into pCO_2^{atm} (Equation 1) water vapour pressure (pH_2O, in atm) was calculated from *in situ* temperature (Tis, in ºC) according to Cooper et al. (1998) (Equation 2). Following Olsen et al. (2003), a decrease of 0.3% from pCO_2^{atm} to fCO_2^{atm} (Weiss, 1974) was considered accurate enough.

$$pCO_2^{atm} = xCO_2^{atm} \cdot (patm - pH_2O) \quad (1)$$

$$pH_2O = 0.981 \cdot \exp(14.32602 - (5306.83/(273.15 + Tis))) \quad (2)$$

Discrete samples were collected at four locations along the commercial track (46±0.3ºN -4.7±0.5ºW; 45.5±0.2ºN -5.6±0.3ºW; 45±0.2ºN -6.7±0.3ºW; 44.5±0.2ºN -7.7±0.3ºW) (*mean*±*standard deviation*) to calibrate the different sensors (Fig. 1). The calibration frequency changed during the ECO project from three per month during 2003 to one per month during 2004.

Alkalinity (A_T) and pH and measurements were done to study the internal consistence of *in situ* fCO_2^{sw} measurements. Poisoned A_T samples, as the DOE handbook (DOE,

1994) recommends, were determined by automatic potentiometric titration with HCl at a final pH of 4.40 (Pérez and Fraga, 1987). The electrodes were standardised using a buffer of pH 4.42 made in CO_2 free seawater (Pérez et al., 2002). The method has an accuracy of ±1 μmol/kg estimated using Certified Reference Material (CRM). The pH samples were kept refrigerated since collection until the spectrophotometric determination following Clayton and Byrne (1993). This method has a precision of 0.00004 and an accuracy (Clayton and Byrne, 1993) of 0.002 (DelValls and Dickson, 1998). The comparison between the *in situ* and the computed fCO_2^{sw} from pH and A_T using the carbonic system constants of Lueker et al. (2000), showed a consistence error of ±6 μatm (n = 365, $r^2 = 0.91$).

Discrete oxygen samples were stored in the dark and analyzed by the Winkler method 24 hours after collection. The potentiometric end-point determination of oxygen has an estimated accuracy of ±2 $\mu mol \cdot kg^{-1}$. Oxygen saturation was calculated following Benson and Krause equation (UNESCO, 1986). The underway fluorescence measurements, determined with a WETLabs fluorometer, were calibrated with chlorophyll extracted by 25mm Whatman GF/F filters and analyzed after 90% acetone extraction in a 10,000 R Turner fluorometer (Yentsch and Menzel, 1963). The precision was ±0.05 $mg \cdot m^{-3}$.

Additionally, the nutrient samples were also collected in polystyrene bottles and stored in the freezer at -30ºC prior to lab analysis. The concentration of nitrate (NO_3), phosphate (PO_4) and silicate ($Si(OH)_4$) were determined by segmented flow analysis with Alpkem autoanalyzers, following Hansen and Grasshoff (1983) with some

175 improvements (Mouriño and Fraga, 1985). The analytical errors are ±0.05 μmol·kg^{-1}
176 for NO_3, ±0.05 μmol·kg^{-1} for $Si(OH)_4$ and ±0.01 μmol·kg^{-1} for PO_4.
177
178 Air-sea CO_2 exchange
179 The exchange of carbon between the atmosphere and the ocean (F) was calculated with
180 the following equation:
181
182 $$F = k\ S\ (fCO_2^{sw} - fCO_2^{atm}) \qquad (3)$$
183
184 Seawater CO_2 solubility (S, mol·L^{-1}·atm^{-1}) was calculated from Weiss (1974) and the
185 piston velocity (k, cm·h^{-1}) was computed from coefficients reported by Nightingale et
186 al. (2000). In spite of the several formulations of piston velocity, the Nightingale's
187 parameterization was pointed out as the more consistent in recent findings (Ho et al.,
188 2006; Sweeney et al., 2007). The wind speed used in our computations was remotely
189 measured by QuikSCAT satellite with temporal and spatial resolutions of 0.25º and 12
190 hours, respectively. This dataset was collected from the Physical Oceanography Active
191 Archive Center of the Jet Propulsion Laboratory (http://podaac.jpl.nasa.gov).
192 Additionally daily mean (average of four measurements per day) of wind vector
193 product was also provided by the NCEP/NCAR reanalysis project (Kalnay et al., 1996)
194 from the web site of the NOAA-CIRES Climate Diagnostics Center, Boulder, Co, USA
195 (http://www.cdc.noaa.gov/). The wind speed from both sources was linearly
196 interpolated at temporal and spatial scale.
197
198 Winter mixed layer

Winter mixed layer (WML) depths were provided by the MERCATOR-OCEAN model (http://www.mercator-ocean.fr) averaging a region of the Bay of Biscay between 44º to 46ºN and between 9º to 4ºW. The WML depth is estimated according to the density criterion establishing the WML lower limit when the density difference is 0.05 $kg \cdot m^{-3}$ from the surface value. This criterion was preferred to the temperature one, following Kara et al., 2000.

RESULTS

Biogeochemical variability

The temporal evolution of the sea surface properties in the Bay of Biscay during the ECO project showed a marked seasonality with two clear seasons, winter and summer (Borja et al., 2000a). The SST pattern (Fig. 2) showed differences between 2003 and 2004 years, with seasonal ranges of 9.1 ºC and 9.5 ºC, respectively. The highest SST values were reached during September 2003 (21.5ºC) and August 2004 (21 ºC) whereas the coldest surface waters were found in February 2003 (12.4ºC) and January 2004 (11.5ºC).

Even though SSS distribution was nearly uniform for the two years (35.617±0.024 (±0.001) psu; Fig. 2), the precipitation–evaporation balance and the meteorological conditions yielded an obvious seasonal pattern. During winter, the surface waters of the Bay of Biscay get usually saltier due to the advection of southern saline waters conveyed northward by the Iberian Poleward Current (Haynes and Barton, 1991). Besides the winter mixing with subsurface saltier waters also contributes to the higher winter SSS. The intensity of both contributions during the ECO cruises showed

224 appreciable differences since the resulting SSS increment was more sustained during
225 winter 2004. Contrary the lowest SSS values were measured during spring achieving
226 absolute SSS minimum, namely, 35.56±0.01 psu, during May 2003. These low SSS
227 values coincided with the thaw period reflecting the influence of runoff from Loire and
228 Garonne rivers that flow with a mean volume of ~2000 $m^3 \cdot s^{-1}$. The intense evaporation
229 during summer and the later stratification breakdown previous to the formation of
230 WML yielded the highest SSS of 35.651±0.021 (±0.004) psu in October 2003.
231
232 The winter convection yielded similar WML maxima during the successive years
233 reaching ~200 m (Fig. 3) at the middle of February and March, respectively. However
234 winter convection during 2004 lasted for almost one more month than in winter 2003.
235 The interannual variations in surface nutrient concentrations are associated with the
236 different vertical mixing pattern. The nutrient maxima (NO_3, PO_4 and $Si(OH)_4$) were
237 2.00, 0.27 and 2.00 $\mu mol \cdot kg^{-1}$ during winter 2003 and 5.51, 0.34 and 2.20 $\mu mol \cdot kg^{-1}$
238 during winter 2004. Besides the quantitative differences, the nutrient ratios were also
239 different for the two winter. The NO_3:$Si(OH)_4$ ratio for 2003 was 1.6 (±0.2) whereas
240 during 2004 it was 3.2 (±0.2) (Table 1). The NO_3:PO_4 ratios also showed interannual
241 variation during the successive winter mixing events reporting 14 (±3) and 18 (±1),
242 respectively. After reaching the maximum winter mixing (February 2003 and April
243 2004), the rapid shoaling of the mixed layer (Lochte et al., 1993) triggered the onset of
244 biological activity leading to complete NO_3 depletion (Fig. 2). On the other hand, the
245 phytoplankton consumption did not cause a total depletion of sea surface PO_4 and
246 $Si(OH)_4$ levels (Fig. 2).
247

A similar temporal evolution was observed for PO_4 and $Si(OH)_4$ concentrations throughout the sampling periods. Both nutrients were gradually reduced during year 2003 reaching minimum values in September. The synthesis – remineralisation balance of organic matter during year 2004 showed different distribution at seasonal scale reporting an intense consumption during the bloom period. The spring bloom – just at the total NO_3 depletion - was extended for a few weeks from the mid February to middle April. The nutrient concentrations during the bloom period kept similar ratios to the prebloom ones, namely, 1.8 (±0.5) and 4.1 (±0.5) for NO_3:$Si(OH)_4$ and 13 (±2) and 20 (±2) for NO_3:PO_4 during 2003 and 2004, respectively (Table 1).

The chl a distribution reached maximum values of 2.6 and 1.2 $mg \cdot m^{-3}$ coinciding the more intense nutrient consumption during March 2003 and April 2004, respectively. Contrary the surface chl a concentration decreased to minimum values due to the nutrient exhaustion during the summer. The breakdown of the summer stratification provoked the upwards input of nutrients to the sea surface reactivating the phytoplankton activity in September.

The oxygen saturation varied from a minimum at the end of the summer period to a maximum just after the bloom periods. The highest saturation values, oversaturation of ~20%, were reached in June 2003 and July 2004 (Fig. 2).

Continuously recordings of fCO_2^{sw}

The seasonal evolution of fCO_2^{sw} (Fig. 2) showed an identical variability with a range of 72 µatm for the two seasonal cycles. Briefly, several features are shared by both annual fCO_2^{sw} cycles. During winter the Bay of Biscay displayed undersaturated

273 fCO_2^{sw} level in relation to atmosphere with an homogeneous value of approximately
274 340 µatm for both winters. After that, minimum fCO_2^{sw} values were registered in spring
275 probably caused by an intense phytoplankton growth. Subsequently, the summer SST
276 increase led the fCO_2^{sw} distribution to the highest values of the seasonal cycle. Finally,
277 during the autumn season fCO_2^{sw} diminished associated to the SST decrease.
278
279 However several events also showed notable differences between both seasonal cycles.
280 Thus the fCO_2^{sw} distribution during winter 2004 increased noticeably until reaching an
281 annual maximum in January 2004 (Fig. 2). This fCO_2^{sw} trend closely followed the
282 evolution of nutrient levels and WML depth even reproducing a rise across two pulses
283 between March and April 2004 (Fig. 2). The biological drawdown also yielded
284 differences in fCO_2^{sw} reaching different undersaturation levels (73 and 85 µatm for
285 2003 and 2004, respectively). For the two seasonal cycles, the recorded spring bloom
286 presented two periods regarding the relationship between fCO_2^{sw} and chl a; one
287 corresponding to peak (February – March) and another to senescent stages (April –
288 May) of phytoplankton growth.
289
290 The fCO_2^{sw} – chl a relationships during the intense CO_2 drawdown reached values of 42
291 (±6) and 60 (±2) $\mu atm \cdot m^3 \cdot mg^{-1}$ during 2003 and 2004 respectively, substantially
292 exceeded the valued registered (~17 $\mu atm \cdot m^3 \cdot mg^{-1}$) by Watson et al. (1991) for the
293 spring bloom in the North Atlantic during the NABE cruises. On the other hand, the
294 photosynthetic activity for the subsequent senescent phase (Table 1) agreed with
295 reported parameters (Watson et al., 1991; Frankignoulle et al., 1996). The
296 thermodynamic control steered the Bay of Biscay surface waters to oversaturated levels

297 of 371 μatm during summer 2003. However the fCO_2^{sw} increase for summer 2004 was
298 not so intense, not exceeding fCO_2^{atm} levels (Fig. 2).
299
300 The influence of the biological processes and the temperature variability on the fCO_2^{sw}
301 distribution during the ECO cruises was evaluated estimating the variables $^{B}fCO_2^{sw}$ and
302 $^{T}fCO_2^{sw}$, respectively, according to Takahashi et al. (2002):
303
304 $$^{B}fCO_2^{sw} = fCO_2^{sw} \exp [0.0423 (SST_{mean} - SST)]$$
305 $$^{T}fCO_2^{sw} = fCO_2^{sw}{}_{mean} \exp [0.0423 (SST - SST_{mean})]$$
306
307 where $^{B}fCO_2^{sw}$ denotes the fCO_2^{sw} normalized to the annual mean SST (SST_{mean}) and
308 $^{T}fCO_2^{sw}$ represents the effect of SST distribution on the annual mean of fCO_2^{sw}
309 ($fCO_2^{sw}{}_{mean}$).
310
311 In other words, $^{B}fCO_2^{sw}$ is the fCO_2^{sw} distribution without the SST control, representing
312 the biological signal as well as other processes such as air-sea exchange and alkalinity
313 variations. The maximum $^{B}fCO_2^{sw}$ values are observed just at the end of the prebloom
314 periods nearly exceeding 403 and 437 μatm in both years. Subsequently the $^{B}fCO_2^{sw}$ is
315 drastically reduced, within a short period of time, due to the onset of phytoplankton
316 CO_2 uptake. Throughout the following months the net biological control reduces the
317 $^{B}fCO_2^{sw}$ in a similar way reaching the annual minima in midsummer, 275 and 279 μatm
318 for 2003 and 2004 respectively. After that heterotrophic processes raise $^{B}fCO_2^{sw}$ to the
319 winter values, establishing seasonal ranges of ~129 and ~159 μatm for 2003 and 2004
320 respectively. Hence, the range of $^{B}fCO_2^{sw}$ for the Bay of Biscay varies between
321 characteristic values of oligotrophic areas (~80 μatm) and typical values of productive

regions (~280 µatm). For the ECO cruises, 78% of the $^{B}fCO_2^{sw}$ variability was explained by the NO_3 distribution ($^{B}fCO_2^{sw}$ = 313(±4) + 55(±7)·NO_3 – 7(±2)·NO_3^2; n=48) showing the strong link between the $^{B}fCO_2^{sw}$ variability and the photosynthesis – respiration processes.

On the other hand, $^{T}fCO_2^{sw}$ distribution, meaning the SST control on fCO_2^{sw} distribution, yielded similar ranges, namely, 145 and 141 µatm with SST amplitude for 9.1 and 9.5ºC for 2003 and 2004.

The monthly average variation of temperature control ($^{T}fCO_2^{sw}$) and biological control ($^{B}fCO_2^{sw}$) are shown in Figure 4b. The combined effect of both controls yields the net fCO_2^{sw} variability (white circles, Fig. 4b). The $^{B}fCO_2^{sw}$ variation reached maximum phytoplankton absorption of ~-46 and ~-73 µatm at the bloom periods of 2003 and 2004 respectively. The biological CO_2 uptake continued throughout the postbloom periods, being clearly evident in autumn 2003 with a reduction of ~35 µatm. The sign of this biological control was inverted from November to February pointing to a dominance of surface heterotrophic processes or CO_2 enrichment due to entrainment of subsurface waters, mainly, during the prebloom 2004. Regarding the variability of the temperature control, the minimum $^{T}fCO_2^{sw}$ was observed during autumn concomitant to the water cooling developed in November 2003. Conversely, during warming periods $^{T}fCO_2^{sw}$ showed higher values steered by SST increase. Maximum values of 58 µatm were reached during both Junes.

The relative magnitude of biological and thermodynamic control was estimated as the ratio of seasonal amplitude of $^{B}fCO_2^{sw}$ and $^{T}fCO_2^{sw}$. The temperature effect played a

similar role for the two years whereas the influence of the processes represented by $^{B}fCO_2^{sw}$ showed an important interannual variability. Thus the fCO_2^{sw} variability associated to the biological control for 2004 was 10% stronger than the thermodynamic component of fCO_2^{sw} variability.

The analysis of the biogeochemical control on fCO_2^{sw} variability was extended performing multiple linear regressions taking into account all the measured variables. The variability of NO_3, PO_4, chl a, SSS and SST are good proxies of the different processes that control the fCO_2^{sw} variability such as thermodynamic effect, remineralization processes and organic matter synthesis. So, the role and percentage of explained fCO_2^{sw} variability by each variable was assessed for the three periods of the seasonal cycle, prebloom (October – February), bloom (March – May) and postbloom (June – September). From here, the relationships considering only the significant variables were established (Table 2).

During the prebloom period, the fCO_2^{sw} distribution was poorly explained (~40%) with a small error of ±6.8 μatm that was associated to its homogeneous distribution from October to February. Water mixing and photosynthetic activity depicted by NO_3 and chl a, respectively, seemed to control the fCO_2^{sw} variation explaining 15% and 21% of fCO_2^{sw} variability, respectively (Table 2). During the bloom period the synthesis of organic matter, represented by PO_4, explained 77% of the total fCO_2^{sw} variability yielding a predicted fCO_2^{sw} error of 10 μatm. In spite of playing a weak role for the other periods, SST was the main factor controlling fCO_2^{sw} trend during the postbloom period explaining ~65% of the total variability. Including every significant variables,

371 the explained variability of fCO_2^{sw} reached 80%, pointing out the prevalence of
372 physical processes during postbloom period.
373
374 Air-sea CO_2 exchange
375 The measurements of fCO_2^{sw} and fCO_2^{atm} (Fig. 2) in the Bay of Biscay indicated a
376 regular absorption of atmospheric CO_2 during the ECO cruises. The fCO_2
377 disequilibrium between seawater and atmosphere was -29±25 (±1) µatm and -36±20
378 (±1) µatm for 2003 and 2004 respectively. The maximum undersaturation of surface
379 waters in relation to the atmosphere was recorded during April 2004, reaching a fCO_2
380 gradient of ~-83 µatm. In contrast, the direction of CO_2 exchange was inverted during
381 August 2003 with an oversaturation of ~9 µatm with respect to the atmosphere.
382
383 The air-sea CO_2 fluxes were computed according to Equation 3, using wind speeds
384 retrieved from remote QuikSCAT sensor and Nightingale's coefficients. The amplitude
385 of daily CO_2 flux ranged from 1.2 to -20 $molC \cdot m^{-2} \cdot yr^{-1}$ (not shown) and the average
386 flux was -1.52±1.89 (±0.08) $molC \cdot m^{-2} \cdot yr^{-1}$ for the ECO cruises (Fig. 5). The net CO_2
387 uptake showed small interannual variability of -1.29±1.68 (±0.09) and -1.7±2.0 (±0.1)
388 $molC \cdot m^{-2} \cdot yr^{-1}$ for 2003 and 2004 respectively. The behaviour of the Bay of Biscay as an
389 atmospheric CO_2 sink was evident throughout every considered partition of the
390 seasonal cycle. The average CO_2 flux was stimulated during both prebloom periods due
391 to kinetic effect of intense winds (Fig. 5), reporting -1.9±1.7 (±0.1) $molC \cdot m^{-2} \cdot yr^{-1}$. The
392 CO_2 uptake for the two bloom periods was only -2.4±2.4 (±0.2) $molC \cdot m^{-2} \cdot yr^{-1}$ in spite
393 of showing the maximum disequilibrium and the absolute maximum of weekly
394 absorption ~-8 $molC \cdot m^{-2} \cdot yr^{-1}$ during the bloom 2004. The small fCO_2 gradient and the
395 weak wind speed during the successive postbloom periods yielded mean CO_2

396 exchanges of -0.08±0.41 (±0.04) and -0.58±0.59 (±0.05) molC·m^{-2}·yr^{-1} for 2003 and
397 2004 respectively.
398
399 Wind speed is one of the main sources of uncertainty in the estimations of CO_2
400 exchange. Therefore the CO_2 fluxes were also estimated using wind speed values from
401 NCEP/NCAR model (Olsen et al., 2003). The known lower celerity of NCEP/NCAR
402 winds (Olsen et al., 2005, Padin et al., 2007b) compared to QuikSCAT values yielded a
403 26% reduction in the annual capacity of CO_2 uptake, though keeping the interannual
404 variability. The annual mean CO_2 uptake in the Bay of Biscay, taking into account the
405 Nightingale's coefficients and wind speed from NCEP/NCAR and QuikSCAT, ranged
406 from -1.3±1.7 (±0.1) molC·m^{-2}·yr^{-1} during 2003 using NCEP/NCAR wind speed and -
407 2.4±2.7 (±0.1) molC·m^{-2}·yr^{-1} during 2004 using QuikSCAT values.
408
409 The empirical relationships developed for each period (see Table 2) were also used to
410 assess the CO_2 exchange in the Bay of Biscay. The disagreements between the *in situ*
411 and modelled CO_2 fluxes are depicted in Figure 5. The mean difference for the entire
412 time series was -0.11±0.51 (±0.02) molC·m^{-2}·yr^{-1} pointing out a slight bias of the
413 estimated algorithms towards fCO_2^{sw} underestimation. The maximum disagreement
414 (~1.81 molC·m^{-2}·yr^{-1}) was observed at the beginning of the postbloom 2004 and in
415 general the CO_2 flux was poorly predicted during postbloom periods. The errors
416 reported during the successive years were ~15 and ~21%, respectively, though there are
417 not too significant due to the reduced CO_2 exchange. On the other hand, the best
418 predictions were achieved during prebloom periods, with an error range of 4–6 %.
419
420 DISCUSSION

The temporal fCO_2^{sw} distribution during the ECO cruises from November 2002 to December 2004 emphasized the biogeochemical differences at seasonal and interannual scale in the inner part of the Bay of Biscay. An abrupt increase of fCO_2^{sw} values was recorded during winter 2004 but still kept the stronger capacity of CO_2 uptake. So, the longer persistence of winter mixing in 2004 provoked a stronger nutrient fertilization that increased in 1.6 times the NO_3 concentration of the previous year and completely modified the nutrients ratios NO_3:PO_4 and NO_3:$Si(OH)_4$ compared to the winter 2003.

The different winter mixing conditions each year determined the development and characteristics of the following periods of the seasonal cycle. For example, the fCO_2^{sw} – chl a relationship showed a significant interannual variability during the bloom periods. The intercept of fCO_2^{sw} – chl a for 2003 was close to the *in situ* fCO_2^{atm} levels as expected (Watson et al., 1991; Frankignouille et al., 1996) pointing out the winter air-sea equilibrium once the biological activity is removed. In contrast the intercept of fCO_2^{sw} – chl a relationship for 2004 appreciably exceeded the in situ fCO_2^{atm} level probably associated with intense winter mixing conditions for the 2004 as we explained below. During the 2004 spring bloom, we have observed a strong CO_2 uptake (~289 µatm) that does not match with the relatively low surface chl a. We suspect that the lower sampling frequency during 2004 could hinder the observation of chlorophyll maximum.

The Eastern North Atlantic Central Waters (ENACW) are formed in the Bay of Biscay by subduction processes during the winter convection when these mode water thermohaline properties are established (Paillet and Mercier, 1997). There is an

interannual variation in these properties as the result of variations in the winter air-sea interaction, oceanic heat transport and eddy activity in the formation area. Consequently the prevailing meteorological conditions were analyzed from October to January for both seasonal cycles in order to investigate the reported differences during the formation period of mode waters. Taking into account the water mass distribution in the vicinity of the Bay of Biscay described by Harvey et al. (1982), the latitudinal module of wind was accumulated throughout the winter mixing period. The results (Figure 3) clearly show two different patterns even though wind speed was nearly the same (8±4 $m \cdot s^{-1}$) for both years. The dominant wind during 2003 was characterized by southern origin (wet and warm) whereas northerly winds (dry and cold) prevailed during the winter mixing of 2004 favouring the longer and deeper winter convection (Pérez et al., 1995). However the nutrient concentrations measured during the ECO cruises even during winter 2004 did not reach the nutrient values previously reported for this region (Treguer et al., 1979; Castro et al., 1998; Pérez et al., 2001). In any case, it seems clear that the meteorological conditions during the formation of the winter mixed layer influence both properties of the mixed layer and their biogeochemical evolution.

The algorithms performed here to predict fCO_2^{sw} for each period fitted the observed variability with an error lower than 10 µatm. Among measured variables, PO_4 played an outstanding role in the fCO_2^{sw} control during bloom periods explaining 77% of fCO_2^{sw} variability. The photosynthetic absorption and respiration processes were adequately depicted by biological utilisation and rapid remineralization of PO_4 in the surface layer. During postbloom periods, the fCO_2^{sw} distribution was mainly led by temperature. This temperature control of 6.9 $\mu atm \cdot {}^{o}C^{-1}$ disagrees with the isochemical

ratio of ~14 $\mu atm \cdot {}^{o}C^{-1}$ estimated from the fCO_2^{sw} variability found in the Bay of Biscay (Takahashi et al., 1993). The influence of processes such as mixing waters and phytoplankton uptake altered the theoretical value as previously described by Lüger et al. (2004) in the Eastern North Atlantic Ocean who reported a temperature control of 8.7 $\mu atm \cdot {}^{o}C^{-1}$. The addition of the nutrient concentration in the assessment of the fCO_2^{sw} algorithm clearly constrains its variability, increasing the fCO_2^{sw} explained variability up to 30%. In fact, compared with previous manuscript where only SST (Stephens et al., 1995; Cosca et al., 2003; Olsen et al., 2004; Feely et al, 2006; Wanninkhof et al., 2006) and chl a (Ono et al., 2004) were considered, we have been able to explain a higher percentage of the fCO_2^{sw} variability with our computed algorithm. Nevertheless, the operational usefulness of the empirical algorithms estimated from nutrients, unlike other computed from SST and chl a, is more limited.

In spite of this interannual variability, the air-sea fluxes reported similar CO_2 uptake during successive years -1.29±1.68 (±0.09) and -1.7±2.0 (±0.1) $molC \cdot m^{-2} \cdot yr^{-1}$ for 2003 and 2004, respectively. From our dataset and using the most frequently used wind speed, we have estimated a CO_2 uptake range from -1.3±1.7 (±0.1) to -2.4±2.7 (±0.1) $molC \cdot m^{-2} \cdot yr^{-1}$ including the value of -1.84 $molC \cdot m^{-2} \cdot yr^{-1}$ for marginal seas between 32ºN and 57ºN (Borges et al., 2005). Extrapolating these CO_2 fluxes to the entire Bay of Biscay – limited by the continental slope, 9ºW meridian and 47ºN parallel; $1.9 \cdot 10^{11}$ m^2 – the absorbing capacity of atmospheric CO_2 varies between 3 and 5 $TgC \cdot yr^{-1}$. These amounts approximately represent 6% and 10% of the CO_2 drawdown estimated for the North Atlantic Ocean between 45º and 55ºN (Telszewski et al., 2005) in spite of standing for only 5% of its area. The intense CO_2 uptake in the Bay of Biscay compared to average values for the North Atlantic Ocean bears relation to the formation of

Eastern North Atlantic Central Water (ENACW). The subduction processes that reach values of 50 -100 $m \cdot yr^{-1}$ (Marshall et al., 1993) isolate CO_2 enriched water during the synthesis and remineralization of organic matter from the surface. Hence the subduction of newly formed ENACW vintages in the Bay of Biscay constitutes a carbon flux to the ocean interior (Marhsall et al., 1993, Follows et al., 1996, Paillet and Mercier, 1997). The oceanic sequestration of atmospheric CO_2 is a decisive process in climatological and geochemical terms (Thiele et al., 1986) therefore its variability, especially in strong sink regions as the Bay of Biscay, should be studied under every climatological conditions.

CONCLUSIONS

The underway measurements performed during the ECO cruises using ships of opportunity from November 2002 to December 2004 report an intense CO_2 uptake in the Bay of Biscay. The estimation of CO_2 fluxes ranged from -1.3 to -2.4 $molC \cdot m^{-2} \cdot yr^{-1}$ on a yearly basis, exceeding the sink capacity of the nearby regions of the North Atlantic Ocean.

The fCO_2^{sw} distribution was correctly predicted from three empirical relationships during prebloom, bloom and postbloom periods reporting errors of ~6.6, ~10 and ~7.7 µatm, respectively. Nevertheless the gathered dataset showed differences in the biogeochemical distributions at seasonal and interannual scale. Thus the intense fertilization in winter 2004 was the trigger mechanism for the strong biological uptake during the following spring bloom, supporting the role of the Bay of Biscay as a CO_2 sink.

Our results highlight the significant effects of physical and biological processes in the uptake capacity of the Bay of Biscay probably steered by meteorological conditions. On the other hand, the use of unattended fCO_2 measuring systems installed on board of ships of opportunity provides valuable information for understanding the CO_2 distribution and the processes affecting its variability at different scales.

546

547 REFERENCES

548

549 Andersen, V., Prieur, L., 2000. One-month study in the open NW Mediterranean Sea
550 (DYNAPROC experiment, May 1995): overview of the hydrobiogeochemical strutues
551 an effects of wind events. *Deep-Sea Research I* 47, 397-422.

552

553 Borges, A.V., Delille, B., Frankignoulle, M., 2005. Budgeting sinks and sources of CO_2
554 in the coastal ocean: Diversity of ecosystems counts. *Geophysical Research Letters* 32,
555 L14601, doi:10.1029/2005GL023053.

556

557 Borja, A., Egaña, J., Valencia, V., Franco, J., Castro, R., 2000. 1947-1997, estudio y
558 validación de una serie de datos diarios de temperatura del agua de mar en San
559 Sebastian, procedente de su Aquarium. *Ozeanografika* 3, 139-152.

560

561 Brewer, P.G., Goyet, C., Friederich, G., 1997. Direct observation of the oceanic CO_2
562 increase revisited. *Proceedings of Natural Academic of Science* 94, 8308-8313.

563

564 Castro, C.G., Pérez, F.F., Holley, S.E., Ríos, A.F., 1998. Chemical characterisation and
565 modelling of water masses in the Northeast Atlantic. *Progress in Oceanography* 41 (3),
566 249-279.

567

568 Clayton, T.D., Byrne, R.H., 1993. Spectrophotometric seawater pH measurements: total
569 hydrogen ion concentration scale calibration of m-cresol purple and at-sea results.
570 *Deep-Sea Research II* 40 (10), 2115-2129.

Cooper, D.J., Watson A.J., Ling, R.D., 1998. Variation of pCO_2 along a North Atlantic shipping route (U.K. to Caribbean): A year of automated observations. *Marine Chemistry* 60, 147-164.

Copin-Montegut, G., Avril, B., 1993. Vertical distribution and temporal variation of dissolved organic carbon in the north-western Mediterranean sea. *Deep-Sea Research II* 40 (10), 1963-1972.

Cosca, C.E., Feely, R.A., Boutin, J., Etcheto, J., McPhaden, M.J., Chavez, F.P., Strutton, P.G., 2003. Seasonal and interannual CO_2 fluxes for the central and equatorial Pacific Ocean as determined from fCO_2-SST relationships. *Journal of Geophysical Research* 108 (C8), 3278, doi:10.1029/2000JC000677.

DelValls, T.A., Dickson, A.G., 1998. The pH of buffers based on 2-amino-2-hydroxymethil-1,3-propanediol ("tris") in synthetic sea water. *Deep-Sea Research I* 45, 1541-1554.

DOE, 1994. Handbook of methods for the analysis of various parameters of carbon dioxide in seawater; version 2. In: Dickson, A.G., Goyet, C. (Eds.), ORNL/CDIAC-74.

Dore, J.E., Lukas, R., Sadler, D.W., Kart, D.M., 2003. Climate-driven changes to the atmospheric CO_2 sink in the subtropical North Pacific Ocean. *Nature* 424 (6950), 754-757.

Feely, R.A., Takahashi, T., Wanninkhof, R., McPhaden, M.J., Cosca, C. E., Sutherland, S.C., 2006. Decadal variability of the air-sea CO_2 fluxes in the equatorial Pacific Ocean. *Journal of Geophysical Research* 111 (C08S90), doi:10.1029/2005JC003129.

Follows, M.J., Williams, R.G., Marshall, J.C., 1996. The solubility pump of carbon in the subtropical gyre of the North Atlantic. *Journal of Marine Research* 54, 605-630.

Frankignoulle, M., Bourge, I., Canon, C., Dauby, P., 1996. Distribution of surface seawater partial CO_2 pressure in the English Channel and in teh Southern Bight of the North Sea. *Continental Shelf Research* 16, 381-395.

Gonzalez-Davila, M., Santana-Casiano, J.M., Rueda, M.J., Llinas, O., Gonzalez-Davila, E.F., 2003. Seasonal and interannual variability of sea-surface carbon dioxide species at the European Station for Time Series in the Ocean at the Canary Islands (ESTOC) between 1996 and 2000. *Global Biogeochemical Cycles* 17 (3), 1076.

Goyet, C., Millero, F., O'Sullivan, D.W., Eischeid, G., McCue, S.J., Bellerby, R.G.J., 1998. Temporal variation of pCO_2 in surface seawater of the Arabian Sea in 1995. *Deep-Sea Research II* 45, 609-623.

Gruber, N., Sarmiento, J.L., Stocker, T.F., 1996. An improved method for detecting anthropogenic CO_2 in the oceans. *Global Biogeochemical Cycles* 10 (4), 809-837.

Gruber, N., 1998. Anthropogenic CO_2 in the Atlantic Ocean. *Global Biogeochemical Cycles* 12, 165-191.

Gruber, N., Keeling, C.D., Bates, N.R., 2002. Interranual variability in the North Atlantic Ocean carbon sink. *Science* 298, 2374-2378.

Hansen, H.P., Grasshoff, K., 1983. Automated chemical analysis. In. K. Grasshoff, M. Ehrhardt and K. Kremling (eds.). Methods of Seawater Analysis. 2nd ed. Verlag Chemie, Weinheim. pp. 368-376.

Harvey, J., 1982. θ-S relationships and water masses in the eastern North Atlantic. *Deep-Sea Research II* 29 (8A), 1021-1033.

Haynes, R., Barton, E.D., 1991. Langranian observations in the Iberian coastal transition zone. *Journal of Geophysical Research* 96 (C8), 14731-14741.

Ho, D.T., Law, C.S., Smith, M.J., Schlosser, P., Harvey, M., Hill, P., 2006. Measurements of air-sea gas exchange at high wind speeds in the Southern Ocean: Implications for global parameterizations. *Geophysical Research Letters* 33, L16611, doi:10.1029/2006GL026817.

Hood, E.M., Merlivat, L., Johannessen, T., 1999. Variations of fCO_2 and air-sea flux of CO_2 in the Greenland sea gyre using high-frequency time series data from CARIOCA drift buoys. *Journal of Geophysical Research* 104 (C9), 20571-20583.

644 Hood, E.M., Merlivat, L., 2000. Annual to interannual variations of fCO_2 in the
645 northwestern Mediterranean Sea: Results from hourly measurements made by
646 CARIOCA buoys, 1995-1997. Journal of Marine Research 59, 113-131.
647
648 Kalnay, E., Kanamitsu, M., Kistler, R., Collins, W., Deaven, D., Gandin, L., Iredell, M.,
649 Saha, S., White, G., Woollen, J., Zhu, Y., Chelliah, M., Ebisuzaki, W., Higgins, W.,
650 Janowlak, J., Mo, K.C., Ropelewski, C., Wang, J., Leetmaa, A., Reynolds, R., Jenne, R.,
651 Joseph, D., 1996. The NCEP/NCAR Reanalysis Project. Bulletin American
652 Meteorological Society 77, 437-471.
653
654 Kara, A.B., Rochford, P.A., Hurlburt, H.E., 2000. An optimal definition for ocean
655 mixed layer depth. Journal of Geophysical Research 105 (7), 16803-16821.
656
657 Körtzinger, A., Kowve, W., Kähler, P., Mintrop, L., 2001. C:N ratios in the mixed layer
658 during productive season in the northeast Atlantic Ocean. Deep-Sea Research I 48, 661-
659 688.
660
661 Le Quere, C., Orr, J.C., Monfray, P., Aumont, O., Madec, G., 2000. Interannual
662 variability of the oceanic sink of CO2 from 1979 through 1997. Global Biogeochemical
663 Cycles 14 (4), 1247-1265.
664
665 Lee, K., Wanninkhof, R., Takahashi, T., Doney, S.C., Feely, R.A. 1998. Low
666 interannual variability in recent oceanic uptake of atmospheric carbon dioxide. *Nature*
667 396, 155-159.
668

669 Lefévre, N., Taylor, A., 2002. Estimating pCO_2 from sea surface temperatures in the
670 Atlantic Gyres. *Deep-Sea Research I* 49, 539-554.
671
672 Lévy, M., Mémery, L., André, J.-M., 1998. Simulation of primary production and
673 export fluxes in the Northwestern Mediterranean Sea. *Journal Marine Research* 56,
674 197-238.
675
676 Lochte, K., Ducklow, H.W., Fasham, M.J.R., Stienen, C., 1993. Plankton succession
677 and carbon cycling at 47ºN 20ºW during the JGOFS North Atlantic Bloom Experiment.
678 *Deep-Sea Research I* 40 (1/2), 91-114.
679
680 Lueker, T.J., Dickson, A.G., Keeling, C.D., 2000. Ocean pCO_2 calculated from
681 dissolved inorganic carbon, alkalinity, and equations for K1 and K2 : validation based
682 on laboratory measurements of CO_2 in gas and seawater at equilibrium. *Marine*
683 *Chemistry* 70, 105-119.
684
685 Luger, H., Wallace, D.W.R., Kortzinger, A., Nojiri, Y., 2004. The pCO_2 variability in
686 the midlatitude North Atlantic Ocean during a full annual cycle. *Global*
687 *Biogeochemical Cycles* 18 (3), GB3023, doi:10.1029/2003GB002200, 2004.
688
689 Maier-Reimer, E., Hasselmann, K., 1987. Tansport and storage of CO_2 in the ocean - an
690 inorganic ocean-circulation carbon cycle model. *Climate Dynamics* 2, 63-90.
691
692 Marshall, J.C., Nurser, A.J.G., Williams, R.G., 1993. Inferring the subduction rate and
693 period over North Atlantic. *Journal of Physical Oceanography* 23, 1315-1329.

694

695 Metzl, N., Poisson, A., Louanchi, F., Brunet, C., Schauer, B., Bres, B., 1995. Spatio-
696 temporal distributions of air-sea fluxes of CO_2 in the Indian and Antarctic Oceans.
697 *Tellus* 47B, 56-69.

698

699 Mouriño, C., Fraga, F., 1985. Determinación de nitratos en agua de mar. *Investigación*
700 *Pesquera* 49, 81-96.

701

702 Nelson, N.B., Bates, N.R., Siegel, D.A., Michaels, A.F., 2001. Spatial variability of the
703 CO_2 sink in the Sargasso Sea. *Deep-Sea Research II* 48, 1801-1821.

704

705 Nightingale, P.D., Malin, G., Law, C.S., Watson, A.J., Liss, P.S., Liddicoat, M.I.,
706 Boutin, J., Upstill-Goddard, R.C., 2000. In situ evaluation of air-sea exchange
707 parameterizations using novel conservative and volatile tracer. *Global Biogeochemical*
708 *Cycles*, 14, 373-387.
709

710 Olsen, A., Bellerby, R.G.J., Johannessen, J., Omar, A.M., Skjelvan, I., 2003.
711 Interannual variaiblity in the wintertime air-sea flux of carbon dioxide in the norhtern
712 Norht Atlantic. *Deep-Sea Research I* 50, 1323-1338.

713

714 Olsen, A., Triñanes, J.A., Wanninkhof, R., 2004. Sea–air flux of CO_2 in the Caribbean
715 Sea estimated using in situ and remote sensing data. *Remote Sensing of Environment* 89
716 (3), 309-325.

717

718 Olsen A., Wanninkhof R., Trinanes J.A., Johannessen T., 2005. The effect of wind
719 speed products and wind speed-gas exchange relationships on interannual variability of
720 the air-sea CO_2 gas transfer velocity. *Tellus B* 57 (2), 95-106.
721

722 Olsen, A., Triñanes, J., Wanninkhof, R., 2004. Sea-air flux of CO_2 in the Caribbean Sea
723 estimated using *in situ* and remote sensing data. *Remote Sensing of Environment* 89,
724 309-325.
725

726 Ono, T., Saino, T., Kurita, N., Sasaki, K., 2004. Basin-scale extrapolation of shipboard
727 pCO_2 data by using satellite SST and Chla. *International Journal of Remote Sensing* 25
728 (19), 3803-3815.
729

730 Padin, X.A., Vázquez-Rodríguez, M., Ríos, A.F., Pérez, F.F., 2007a. Atmospheric CO_2
731 measurements and error analysis on seasonal air-sea CO_2 fluxes in the Bay of Biscay.
732 *Journal of Marine Systems*, doi:10.1016/j.jmarsys.2006.05.010.
733

734 Padin, X.A., Vázquez-Rodríguez, M., Ríos, A.F., Pérez, F.F., 2007b. Surface CO_2
735 measurements in the English Channel and Southern Bight of North Sea using voluntary
736 observing ships. *Journal of Marine Systems*, doi:10.1016/j.jmarsys.2006.05.011.
737

738 Paillet, J., Mercier, H., 1997. An inverse model of the eastern North Atlantic general
739 circulation and thermocline ventilation. *Deep-Sea Research II* 44 (8), 1293-1328.
740

741 Pérez, F.F., Fraga, F., 1987. A precise and rapid analytical procedure for alkalinity
742 determination. *Marine Chemistry* 21, 169-182.

Pérez, F.F., Ríos, A.F., King, B.A., Pollard, R.T., 1995. Decadal changes of the θ-S relatioship of the Eastern North Atlantic Central Water. *Deep-Sea Research II* 42 (11/12), 1849-1864.

Pérez, F.F., Castro, C.G., Álvarez-Salgado, X.A., Ríos, A.F., 2001. Coupling between the Iberian basin-scale circulation and the Portugal boundary current system: a chemical study. *Deep-Sea Research I* 48, 1519-1533.

Pérez, F.F., Alvarez, M., Ríos, A.F., 2002. Improvements on the back-calculation technique for estimating anthropogenic CO_2. *Deep-Sea Research I* 49 (5), 859-875.

Peylin, P., Rayner, P.J., Bousquet, P., Carouge, C., Hourdin, F., Heinrich, P., Ciais, P., 2005. Daily CO_2 flux estimates over Europe from continuous atmospheric measurements: 1, inverse methodology. *Atmospheric Chemistry and Physics* 5, 3173-3186.

Sabine, C.L., Feely, R.A., Gruber, N., Key, R.M., Lee, K., Bullister, J.L., Wanninkhof, R., Wong, C.S., Wallace, D.W.R., Tilbrook, B., Millero, F.J., Peng, T.H., Kozyr, A., Ono, T., Rios, A.F., 2004. The oceanic sink for anthropogenic CO_2. *Science* 305 (5682), 367-371.

Sarmiento, J.L., 1995. Modeling the oceanic uptake of anthropogenic carbon. U.S. JGOFS News: 4-6.

768 Sarmiento, J.L., Sundquist, E.T., 1992. Revised budget for the oceanic uptake of
769 anthropogenic carbon dioxide. *Nature* 356, 589-593.
770
771 Stephens, M.P., Samuels, G., Olson, D.B., Fine, R.A., Takahashi, T., 1995. Sea-air flux
772 of CO_2 in the north Pacific using shipboard and satellite data. *Journal of Geophysical*
773 *Research* 100 (C7), 13571-13583.
774
775 Sweeney, C., Gloor, E.M., Jacobson, A.R., Key, R.M., Galen, M., Sarmiento, J.F. and
776 Wanninkhof, R. 2007. Constraining Global air-sea Gas Exchange for CO_2 with recent
777 Bomb ^{14}C measurements. *Global Biogeochemical Cycles* 21 (2), GB2015,
778 doi:10.1029/2006GB002784.
779
780 Takahashi, T., Feely, R.A., Weiss, R.F., Wanninkhof, R.H., Chipman, D.W., 1997.
781 Global air-sea flux of CO_2: An estimate based on measurements of sea-air pCO_2
782 difference. *Proceedings of Natural Academic of Science* 94, 8292-8299.
783
784 Takahashi, T., Olafsson, J., Goddard, J.G., Chipman, D.W., Sutherland, S.C., 1993.
785 Seasonal variation of CO_2 and nutrients in the high-latitude surface oceans: a
786 comparative study. *Global Biogeochemical Cycles* 7 (4), 843-878.
787
788 Takahashi, T., Sutherland, S.C., Sweeney, C., Poisson, A., Metzl, N., Tilbrook, B.,
789 Bates, N., Wanninkhof, R., Feely, R.A., Sabine, C., Olafsson, J., Nojiri, Y., 2002.
790 Global Sea-Air CO_2 flux based on climatological surface ocena pCO_2 and seasonal
791 biological and temperature effects. *Deep-Sea Research II* 49, 1601-1622.
792

Tans, P. P., Fung, I. Y., Takahashi, T., 1990. Observational Constraints on the global atmospheric CO_2 budget. *Science* 247, 1431-1438.

Telszewski, M., Schuster, U., Watson, A.J., Olsen, A., Johannessen, T., Gonzalez-Davila, M., Steinhoff, T., Wallace, D.W.R., Körtzinger, A., 2006. Variability of the CO_2 air-sea exchange on a seasonal scale in the North Atlantic derived from shipboard measurements in 2005. IP CARBOOCEAN report (deliverables D4.3 and D4.4).

Treguer, P., Le Corre., P., Grall, J.R., 1979. Seasonal variations of nutrients in the upper waters of the Bay of Biscay and their relation to phytoplankton growth. *Deep-Sea Research I* 26 (10), 1121-1152.

Unesco, 1986. Progress on oceanographic tables and standards 1983-1986. Work and recomendations of UNESCO/SCOR/ICES/IAPSO Joint panel. UNESCO Technical Papers in Marine Science 50.

Wallace, D.W.R., 1995. Monitoring global ocean carbon inventories. Ocean Observing System Development Panel, OOSDP Background Report No. 5, Texas A&M University, College Station, TX, 54pp.

Wanninkhof, R., Olsen, A., Trinanes, J., 2007. Air-sea CO_2 fluxes in the Caribbean Sea from 2002-2004. *Journal of Marine Systems* 66 (1), 272-284.

816 Watson, A.J., Robinson, C., Robinson, J.E., Williams, P.J. le B., Fasham, M.J.R., 1991.
817 Spatial variability in the sink for atmospheric carbon dioxide in the North Atlantic.
818 *Nature* 350, 50-53.
819
820 Weiss, R.F., 1974. Carbon dioxide in water and seawater: the solubility of non-ideal
821 gas. *Marine Chemistry* 2, 203-215.
822
823 Yentsch., C.S., Menzel, D.W., 1963. A method for the determination of phytoplankton
824 chlorophyll and phaeophytin by fluorescence. *Deep-Sea Research* 10 (3), 221-231.
825
826
827
828
829
830
831
832
833
834
835
836
837
838
839
840

841 FIGURE CAPTIONS

842

843 Figure 1: Map of the study area showing the regular route (black line) and the four
844 sampling stations (white circles) in the inner part of the Bay of Biscay.

845

846 Figure 2: Mean values of the four stations during each cruise of sea surface temperature
847 (SST; white circles), sea surface salinity (SSS; grey circles), phosphate (PO_4; white
848 circles), silicate ($Si(OH)_4$; grey circles) and nitrate concentration (NO_3; dark grey
849 circles), chlorophyll *a* concentration (chl a; white circles), oxygen (O_2; grey circles) and
850 CO_2 fugacity in the seawater (black circles) and the atmosphere (dotted line).

851

852 Figure 3: Mixed layer depth throughout the following 215 days from 1st October of the
853 winter mixing period of 2003 (black line) and 2004 (grey line) estimated from
854 MERCATOR-OCEAN model. Accumulated latitudinal component of wind speed
855 during the same period retrieved from QuikSCAT sensor at averaged point (45ºN 6ºW)
856 during 2003 (white circle) and 2004 (grey circle).

857

858 Figure 4: a) Average values of the four stations of chlorophyll *a* concentration (white
859 circles) and the monthly distribution of fCO_2^{sw} at the mean sea surface temperature at
860 annual scale ($^{B}fCO_2^{sw}$, black circles) and the annual mean fCO_2^{sw} value corrected for
861 changes in temperature ($^{T}fCO_2^{sw}$, grey circles). b) Average values of observed fCO_2^{sw}
862 (white circles) for each ECO transect in the Bay of Biscay and monthly variation of
863 $^{B}fCO_2^{sw}$ meaning biological control (black bar) and $^{T}fCO_2^{sw}$ meaning temperature
864 control (grey bar).

865

Figure 5: Interpolated values from weekly averages of air-sea CO_2 flux estimated in the Bay of Biscay (thick line) and of flux anomalies associated to fCO_2^{sw} estimation using empirical relationships (fine line) as well as mean values for each period and for the entire sampled period. Interpolated values of wind speed obtained from QuikSCAT sensor (grey thick line) and NCEP/NCAR reanalysis model (grey fine line).

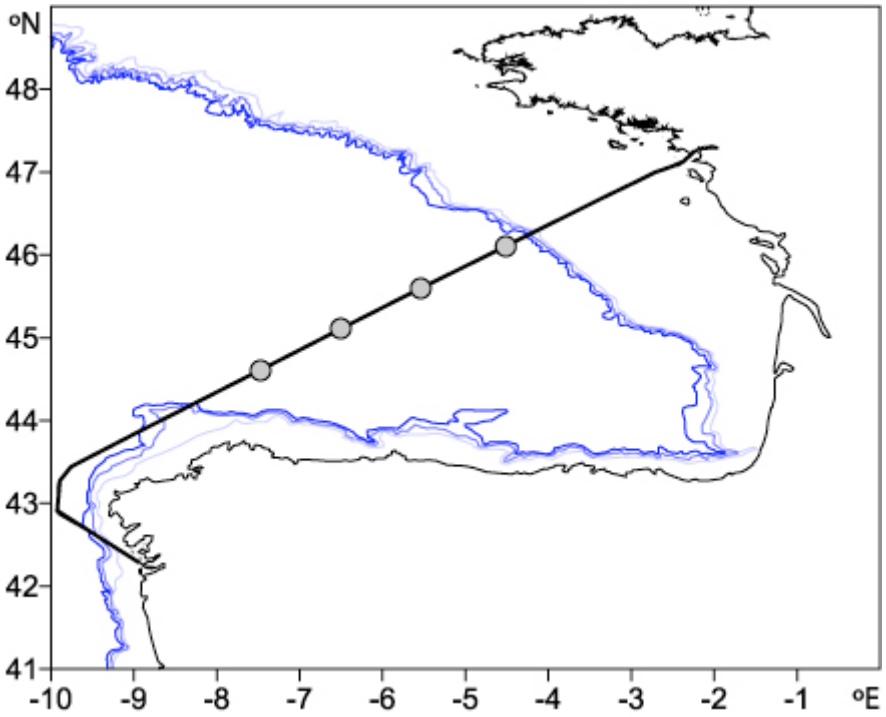

Figure 1

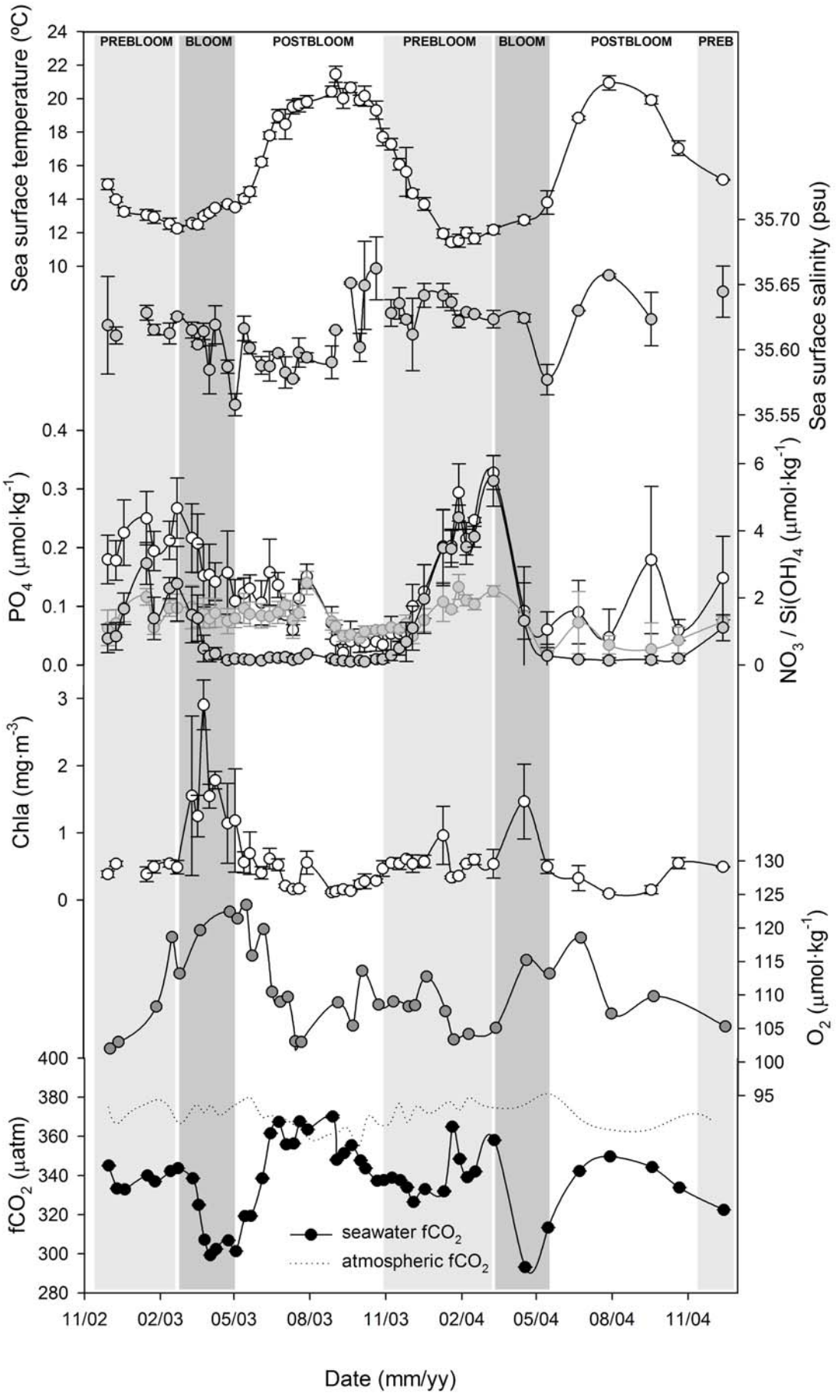
PREBLOOM
BLOOM
POSTBLOOM
PREBLOOM
BLOOM
POSTBLOOM
PREB
Sea surface temperature (ºC)
Sea surface salinity (psu)
PO4 (µmol·kg-1)
NO3 / Si(OH)4 (µmol·kg-1)
Chla (mg·m-3)
O2 (µmol·kg-1)
fCO2 (µatm)
seawater fCO2
atmospheric fCO2
11/02
02/03
05/03
08/03
11/03
02/04
05/04
08/04
11/04
Date (mm/yy)

925

926 Figure 2

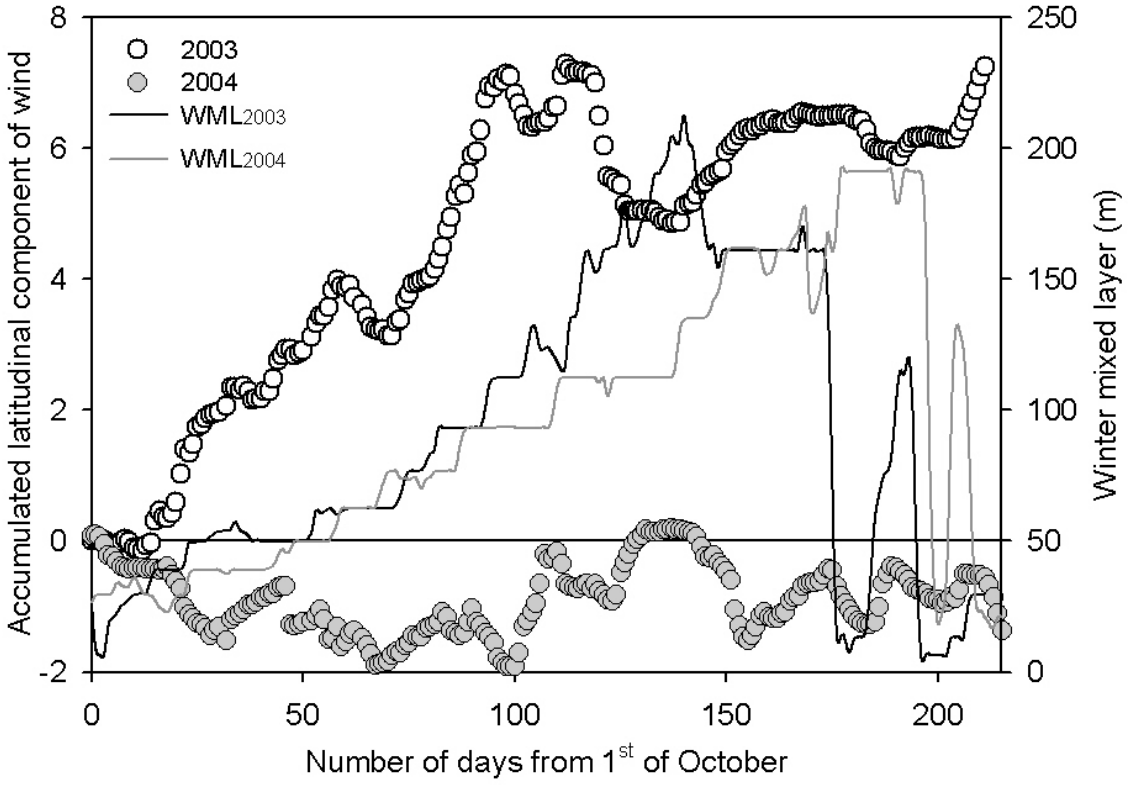

927

928

929 Figure 3

930

931

932

933

934

935

936

937

938

939

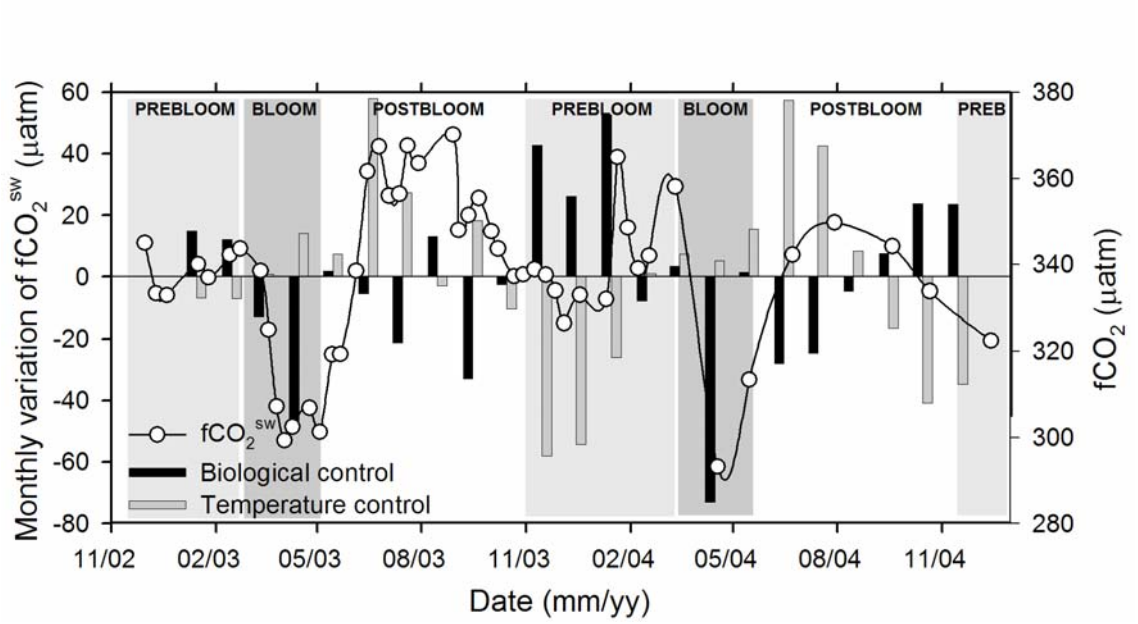
PREBLOOM
BLOOM
POSTBLOOM
PREBLOOM
BLOOM
POSTBLOOM
PREB
Monthly variation of fCO2 sw (µatm)
fCO2 (µatm)
fCO2 sw
Biological control
Temperature control
Date (mm/yy)
11/02
02/03
05/03
08/03
11/03
02/04
05/04
08/04
11/04

Figure 4

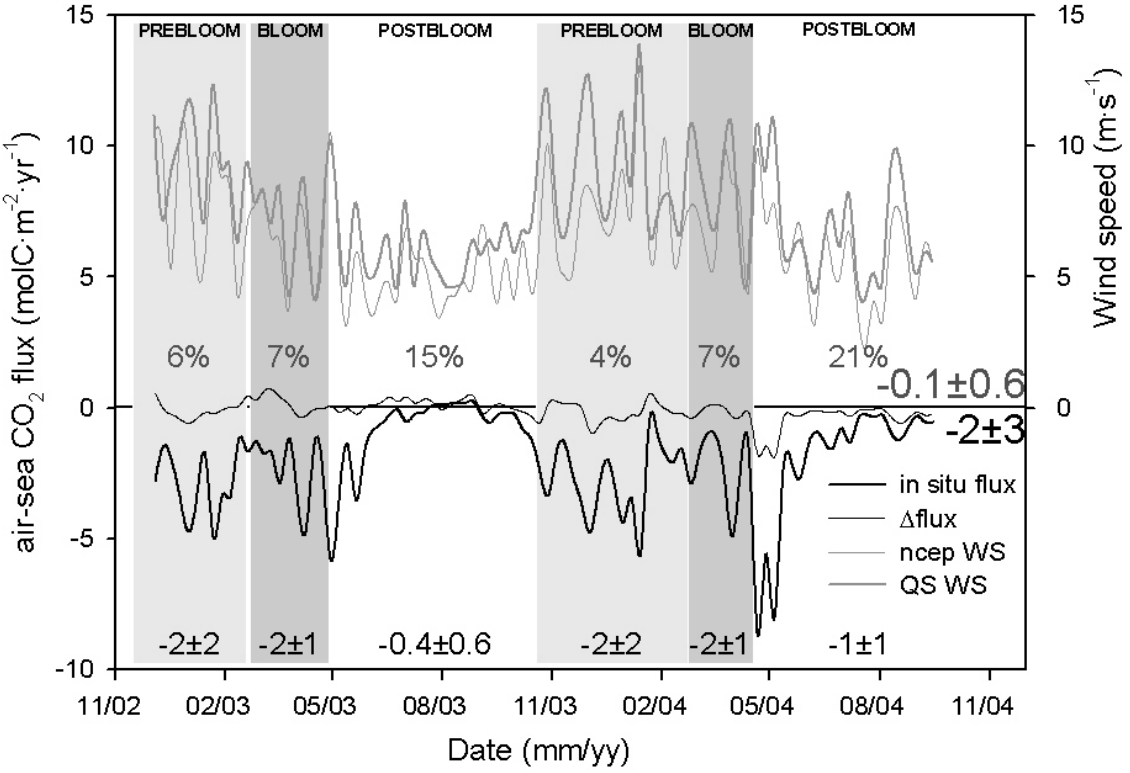
PREBLOOM
BLOOM
POSTBLOOM
PREBLOOM
BLOOM
POSTBLOOM
15
10
5
0
-5
-10
air-sea CO_2 flux (molC·m^{-2}·yr^{-1})
Wind speed (m·s^{-1})
6%
7%
15%
4%
7%
21%
-0.1±0.6
-2±3
in situ flux
Δflux
ncep WS
QS WS
-2±2
-2±1
-0.4±0.6
-2±2
-2±1
-1±1
11/02
02/03
05/03
08/03
11/03
02/04
05/04
08/04
11/04
Date (mm/yy)

Figure 5

964
965